

***Ab initio* (GaAs)₃(AlAs)₃ (001) superlattice calculations: Band offsets and formation enthalpy**

D. M. Bylander and Leonard Kleinman

Department of Physics, The University of Texas, Austin, Texas 78712

(Received 23 December 1986; revised manuscript received 11 May 1987)

We have performed self-consistent semirelativistic *ab initio* pseudopotential calculations of the (GaAs)₃(AlAs)₃ (001) superlattice. The valence-band offset is obtained by adding the energy of the top of the valence band relative to the average crystal potential in bulk GaAs and AlAs to the average crystal potential in the central sections on both sides of the superlattice. The 0.446-eV offset obtained is in good agreement with current experimental values. The formation enthalpy of the three-layer superlattice is found to be 1.2 meV (per twelve-atom unit cell) in comparison with 14.9 meV for the monolayer superlattice (per four-atom unit cell); this is attributed to a Coulomb repulsion between the interfacial planes.

I. INTRODUCTION

Measurements of the valence-band offset in GaAs-AlAs superlattices have been made with increasing frequency over the past dozen years. (We include results obtained from GaAs-Al_xGa_{1-x}As superlattices; even though the gaps are nonlinear in x , the ratio $\Delta E_v/\Delta E_g$ appears to be independent of x). The original measurement¹ gave $\Delta E_v=0.183$ eV and as recently as 1983 a value of 0.19 eV was listed.² Most recently, however, values of 0.43, 0.45, 0.47, and 0.56 eV have been reported.³⁻⁶

Because the average Coulomb potential in an infinite crystal is undefined, attempts to calculate band offsets from the properties of the constituent crystals are at best *ad hoc*. One of the earliest assumptions made⁷ was that the conduction-band offset ΔE_c is equal to the difference in electron affinities. This would be true if zinc-blende surfaces did not reconstruct and if the superlattice interfacial electronic charge distribution were a sum of the constituent crystal surface charge densities. Using $\Delta E_v=\Delta E_g-\Delta E_c$ and the affinities of Ref. 7 yields $\Delta E_v=0.075$ eV. Frensely and Kroemer⁸ suggested that the top of the valence band in each of the constituent crystals should be calculated with respect to the average of the potentials at the two zinc-blende empty lattice sites. They obtained $\Delta E_v=0.26$ eV, but using their model and the results of this calculation we get 0.177 eV. Harrison's bond orbital method which is essentially a simplified tight-binding calculation in which diagonal matrix elements are taken equal to atomic eigenvalues results in⁹ $\Delta E_v=0.04$ eV. Van de Walle and Martin¹⁰ set the arbitrary zero of Coulomb potential by superposing atomic Coulomb potentials. This resulted in $\Delta E_v=0.60$ eV. Note, however, that

$$V_{000}^{\text{atom}} = -(8\pi^2/3) \int \rho(r)r^4 dr$$

so that this zero of potential is very sensitive to the long-range tails of the atomic charge densities. Thus their result must have a strong dependence on whether the Latter correction¹¹ is included in the atomic calculation or whether any s to p promotion has been included in the atomic configurations. Tersoff¹² argues that interface

states screen interface dipoles and that this results in the equilibration of effective midgap energies (defined as that energy where valence- and conduction-band contributions to a Green's function become equal). Because of the similarity of GaAs and AlAs, it is almost certain that interface states do not exist in this superlattice; if they do, their decay length must be¹³ well over 140 Å. On the other hand, the interface double layer, about which we shall have much more to say later, has a total width of no more than 4 Å. In spite of this and other inconsistencies discussed by Tersoff¹² himself, ΔE_v 's of 0.35 and 0.55 eV are obtained for GaAs-AlAs (depending on a choice made for correcting GaAs conduction-bands' position relative to the valence bands) and equally good results are obtained for other superlattices. Thus we cannot exclude the possibility that the equilibration of Tersoff's or some other similarly defined effective midgap energies may play an important role in determining band offsets, although probably not for the reason given by Tersoff.

Ab initio superlattice calculations therefore are of interest not only to obtain numerical values for band offsets, but also to try to obtain some insight (via a study of the electronic charge redistribution, etc.) into why some of the simple models work as well as they do. *Ab initio* calculations are also required to obtain the formation enthalpy,¹⁴ a quantity of some importance in understanding the stability of the superlattice. Pioneering first-principles calculations were performed by Van de Walle and Martin¹⁵ on several superlattices including (GaAs)₃(AlAs)₃ (001) and (110). They obtained $\Delta E_v=0.35$ eV (for both) and estimated inaccuracies of 0.05 eV in the calculation due to the small number of layers in the superlattice, finite number of plane-wave basis functions, and finite sampling of the Brillouin zone (BZ). We note that their 6-Ry cutoff in plane-wave kinetic energy, while corresponding to about 500 plane waves in the superlattice, corresponds to only 65 plane waves for the Γ_{15} states in zinc-blende. A much earlier calculation by Pickett, Louie, and Cohen¹⁶ failed to be first principles only in that they used empirical rather than *ab initio* pseudopotentials. They obtained $\Delta E_v=0.25$ eV. The empirical pseudopotential is well defined only for zinc-blende reciprocal-lattice vectors so

that some error is made in extrapolating it to the very small superlattice reciprocal-lattice vectors. The major source of error in that calculation, however, is probably due to lack of convergence. Their superlattice was much thicker than necessary to calculate band offsets so that their 1180-plane-wave expansion is actually less converged than the 500-plane-wave expansion of Ref. 15.

In this paper we perform Gaussian orbital calculations of the $(\text{GaAs})_3(\text{AlAs})_3$ (001) superlattice valence-band offset and formation enthalpy. The computational method is discussed in the next section and the accuracy of the basis set indicated by comparing a monolayer superlattice formation-enthalpy calculation with our¹⁴ recent mixed-basis-set calculation. In the third section we present our results for the three-layer superlattice and discuss them in some detail.

II. COMPUTATIONAL METHOD

The monolayer superlattice calculation described here is identical in every respect to the calculation of Ref. 14 except for the basis sets used. The three-layer superlattice calculation is then made as identical as possible to the monolayer calculation. For example, the charge density and exchange-correlation potential are calculated at three times as many points and fit with three times as many plane waves plus the same set of Gaussian fitting functions on each atom.¹⁷ Thus, except for the fact that larger numbers must be subtracted to obtain the formation enthalpy, the three-layer superlattice calculation has the same accuracy as the monolayer Gaussian orbital calculation. The 12 000 fitting points are obtained by taking the randomly generated points of the zinc-blende unit cells plus those equivalent zinc-blende points obtained by threefold rotations which become inequivalent in the superlattice and repeating the zinc-blende cell six times for the superlattice. The mixed basis set¹⁴ consisted of all plane waves with $k^2 < 19.3(2\pi/a)^2$, corresponding to 89 plane waves for the Γ_{15} states in zinc-blende, plus two s and two p Gaussian orbitals on each atomic site. This basis set is obviously superior to the plane-wave basis set used in Ref. 15; it is also too large to be practical for a three-layer superlattice. It is our aim to convince the reader that the Gaussian orbital basis set, which is quite practical for the three-layer superlattice, is only slightly inferior to the mixed basis set. It should be pointed out that it is fairly tedious to obtain the Gaussian exponents so that the method is too time consuming for a survey of seven different superlattices as presented in Ref. 15. The Gaussian exponents listed in Table I were obtained by actually calculating the total energies of GaAs and AlAs and minimizing them as a function of the Gaussian exponents. The calculations were performed using the two- k -point sample $(2\pi/a)(\frac{1}{4}, \frac{1}{4}, \frac{1}{4})$ and $(2\pi/a)(\frac{1}{4}, \frac{1}{4}, \frac{3}{4})$. To

reduce the number of parameters to a practical number, we required the s and p Gaussians to have the same even tempered set of four exponents. In addition, we included a single d Gaussian on each atom for a total of nine (three per atom) independent parameters. We, of course, required the same As exponents (at a cost of about 5 meV) in both GaAs and AlAs. The equality of the long-range exponents for all three atoms shown in Table I was not forced.

In Table II we compare the two- k -point and twelve- k -point¹⁸ Gaussian orbital results for the equilibrium lattice constant, cohesive energy, and bulk modulus of GaAs and AlAs as well as the monolayer superlattice formation enthalpy with the twelve- k -point mixed-basis-set results of Ref. 14. Small errors of the order of 1 meV in Ref. 14 arising from inconsistencies in the random fitting points have been corrected. Note that the formation enthalpy¹⁹ increases by only 5.6 meV on going from the 2- to 12-point sample; however, had we subtracted the two-point superlattice cohesive energy from the sum of the 12-point GaAs and AlAs cohesive energies the increase would have been 296.5 meV. Thus we see that for calculating the formation enthalpy and presumably for band offsets, a small k -point sample is satisfactory providing the same set of k -points is used for the superlattice and constituent crystals. We see that the Gaussian basis set actually results in a 14.3-meV better converged GaAs cohesive energy²⁰ than the mixed basis set, while for AlAs it is 24.2 meV worse.

After this paper was completed we performed essentially converged monolayer superlattice calculations using all $k^2 < 33.5(2\pi/a)^2$, corresponding to 181 Γ_{15} zinc-blende plane waves, plus two s and two p Gaussians. In a similar calculation for Si we²¹ found that replacing the longer-range p Gaussian with a d Gaussian increased the cohesive energy by 40 meV but for GaAs and AlAs it reduced it by a fraction of an meV, even though with so many plane waves the longer-range p Gaussian only contributes about 2 meV to the convergence. We found that the converged calculation increased the GaAs cohesive energy by 75.9 meV and the AlAs by 62.0 meV relative to the earlier mixed-basis-set calculation. It increased the monolayer superlattice cohesive energy by 132.3 meV, that is by 5.6 meV less than the sum of the GaAs and AlAs increases, resulting in a converged monolayer superlattice formation enthalpy of 15.5 meV. Thus although our Gaussian basis set is on the average not quite as converged as the smaller mixed basis set, its convergence is more even, resulting in a formation enthalpy within 0.4 meV of the fully converged result. In order to have a rough estimate of convergence errors in the valence-band-offset calculation, we note that the GaAs Γ_{15} state converged by 2.8 meV and the AlAs by 11.3 meV on going from the small to large mixed basis sets.

TABLE I. Gaussian basis function exponents (in bohr⁻²). The first four exponents are for s and p orbitals; the last, in parentheses for d orbitals.

Ga	0.12	0.3470	1.0035	2.902	(0.25)
Al	0.12	0.3194	0.8502	2.263	(0.33)
As	0.12	0.3781	1.1916	3.755	(0.29)

TABLE II. Comparison of experiment and three calculations of GaAs and AlAs equilibrium bond lengths, cohesive energies, bulk moduli, and (GaAs)₁(AlAs)₁ formation enthalpy. The calculations are with a mixed basis set using a 12-**k**-point BZ sample, and with a Gaussian basis set using 2- and 12-**k**-point samples.

	GaAs				AlAs			
	Expt.	Mixed	Calc. 2k	12k	Expt.	Mixed	Calc. 2k	12k
a_0 (Å)	5.6533	5.6595	5.6640	5.6548	5.6611	5.6688	5.6787	5.6696
E_{coh} (eV)	6.7	7.6996	7.5445	7.7139	7.7	8.5475	8.4057	8.5233
B (10^{11} cgs)	7.55	7.28	7.20	7.20	7.81	7.30	7.43	7.34
		(GaAs) ₁ (AlAs) ₁						
	Mixed	2k	12k					
Formation enthalpy (meV)	10.9	9.5	15.1					

In order to have a common arbitrary zero of Coulomb potential, both calculations were performed using the same potential (which was self-consistent for the smaller basis set). This implied 8.5 meV increase in valence-band offset would be expected to be partially screened by changes in the interfacial charge distribution if a fully converged three-layer superlattice calculation were possible; thus it represents an upper limit to the estimated error.

III. RESULTS

The contributions to the cohesive energy of the three-layer superlattice listed in Table III are obtained in exactly the same way as those for the monolayer superlattice were in Ref. 14 except for the change in basis set. The Gaussian basis set results in 252×252 complex Hamiltonian matrices [$(4s + 4 \times 3p + 1 \times 5d)$ orbitals on each of 12 atoms in the unit cell]. The lattice constant was taken to be the average of the calculated (twelve-**k**-point) equilibrium GaAs and AlAs values listed in Table II. The $\frac{1}{16}$ th irreducible wedge of the BZ was sampled at the six **k**-points (in units of $2\pi/a$) $(\frac{1}{8}, \frac{1}{8}, \frac{1}{12})$, $(\frac{1}{8}, \frac{3}{8}, \frac{1}{12})$,

$(\frac{3}{8}, \frac{3}{8}, \frac{1}{12})$, $(\frac{1}{8}, \frac{5}{8}, \frac{1}{12})$, $(\frac{3}{8}, \frac{5}{8}, \frac{1}{12})$, and $(\frac{1}{8}, \frac{7}{8}, \frac{1}{12})$. This is equivalent to an 18-point sample for the monolayer superlattice (to these six points add those obtained by replacing $k_z = \frac{1}{12}$ with $k_z = \frac{3}{12}$ and $\frac{5}{12}$) and therefore we recalculated the monolayer superlattice cohesive energy with the 18-point sample and found only 0.1 meV change from the 18-point sample. Thus we may once and forever assume our BZ sample is converged.

In order to check the dependence of our results on the use of the random fitting points we generated two other random point sets and used the set which gave the larger discrepancy in the sum of the GaAs and AlAs cohesive energies to recalculate the $n=3$ superlattice formation enthalpy. We obtained the 0.0007 eV shown in Table III, 1.0 meV smaller than the original result. For the $n=1$ superlattice the decrease was about $\frac{1}{3}$ as large, from 15.1 to 14.7 meV. We take the average of the results from the two sets of fitting points to be our final result. Thus we find a 1.2-meV formation enthalpy for the 12-atom unit cell of the $n=3$ superlattice to be compared with a 14.9-meV formation enthalpy for the four-atom unit cell of the monolayer superlattice. The 6.85 meV per interface²² re-

TABLE III. Four contributions to the total energy of (GaAs)₃(AlAs)₃ (001) at a lattice constant $a = 5.6622$ Å and its cohesive energy and formation enthalpy all calculated with the Gaussian basis set using two different sets of fitting points. Note that the formation enthalpy is defined as minus the heat of formation.

	Set I	Set II
$\sum_{nk} \epsilon_{nk} - \sum_{\mathbf{K}} V(\mathbf{K}) \rho(\mathbf{K})$ (Ry)	23.495 903	23.495 804
$\frac{1}{2} 8\pi\Omega \sum_{\mathbf{K}} \rho^2(\mathbf{K}) / K^2$ (Ry)	9.332 236	9.332 411
$\int [\epsilon_{xc}(\rho_T) \rho_T - \sum_c \epsilon_{xc}(\rho_c) \rho_c] d^3r$ (Ry)	-36.439 433	-36.438 270
E_{Ewald} (Ry)	-100.902 834	-100.902 834
E_{total} (Ry)	-104.514 128	-104.512 889
E_{atom} (Ry)	-100.933 842	-100.933 842
E_{coh} (eV)	48.7098	48.6929
$3(E_{\text{coh}}^{\text{GaAs}} + E_{\text{coh}}^{\text{AlAs}})$ (eV)	48.7115	48.6936
Formation enthalpy (eV)	0.0017	0.0007

quired to change the interfacial separation from $3a/2$ to $a/2$ we attribute to a Coulomb repulsion between interfaces.

In Fig. 1 we plot contours of constant $\Delta\rho$, the difference between the superlattice charge density and that of its bulk constituents. By its very definition, then, $\Delta\rho$ is discontinuous at the interfacial plane. The plots are in two (100) planes, one containing As atoms and the other Ga and Al. The interfacial As atoms bond with both Al and Ga atoms. In order to see both these bonds in a single picture, in Fig. 2 we plot $\Delta\rho$ in the (011) plane. This plane cuts the interfacial (001) plane at 45° . The $\Delta\rho$ contours are much more complicated than might have been expected. The AlAs interfacial bond gains charge and the GaAs bond loses it, but away from the bonding direction the charge flow across the interface is in the opposite direction so that there is a net flow across the interface from the Al side to the Ga side. This is easily observed to be the case in Fig. 3 where the planar average of the difference between the superlattice charge density and that of its bulk constituents is plotted. The maximum $\Delta\rho$ in Fig. 2 along the bonding and nonbonding directions represents changes of 0.18% and 0.33%, respectively. Note that although the midplane between interfaces is not a reflection plane, for the charge contours plotted in the GaAl (100) plane of Fig. 1 and the bond-containing plane of Fig. 2 it is. Thus in these planes, like charge on neighboring interfaces is closest to like charge. In the As (100) plane of Fig. 1 one sees that negative lobes project from the As interfacial atoms into

the GaAs and on both sides of these lobes are even larger positive contours. In one- and three-layer superlattices the As atoms in neighboring interfaces are offset from one another so that the left-hand positive contours on an As atom in one interface are almost directly opposite the right-hand positive contours on an As atom in the neighboring interface.

Complementing the Coulomb repulsion between interfaces is a weaker attractive interaction. The source of this attraction is identical to that between two real surfaces separated by a very short distance, i.e., the tunneling of eigenfunctions from a medium, through an intervening medium, back into the original medium. We have examined the 24 (neglecting spin degeneracy) valence eigenfunctions of our 12-atom unit cell at $\mathbf{k}=(2\pi/a)(\frac{1}{8}, \frac{1}{8}, \frac{1}{12})$ and found eight, which are plotted in Fig. 4, show fairly strong signs of localization while another six show slightly weaker signs. Note that except for the highest and lowest states these all lie in an energy range common to the valence bands of both GaAs and AlAs and therefore in a thick superlattice will not be absolutely localized, but will be strongly resonant in one of the constituents.

Figure 5 is a plot of the planar average of the local potential of the superlattice. It includes all contributions to the potential except the nonlocal part of the pseudopotential. Because our pseudopotentials are split in a somewhat arbitrary manner into local and nonlocal parts,²³ no physical significance can be attached to this figure. Indeed, we find the \bar{V} of AlAs to lie 0.8383 eV below that of GaAs (where \bar{V} is the average potential

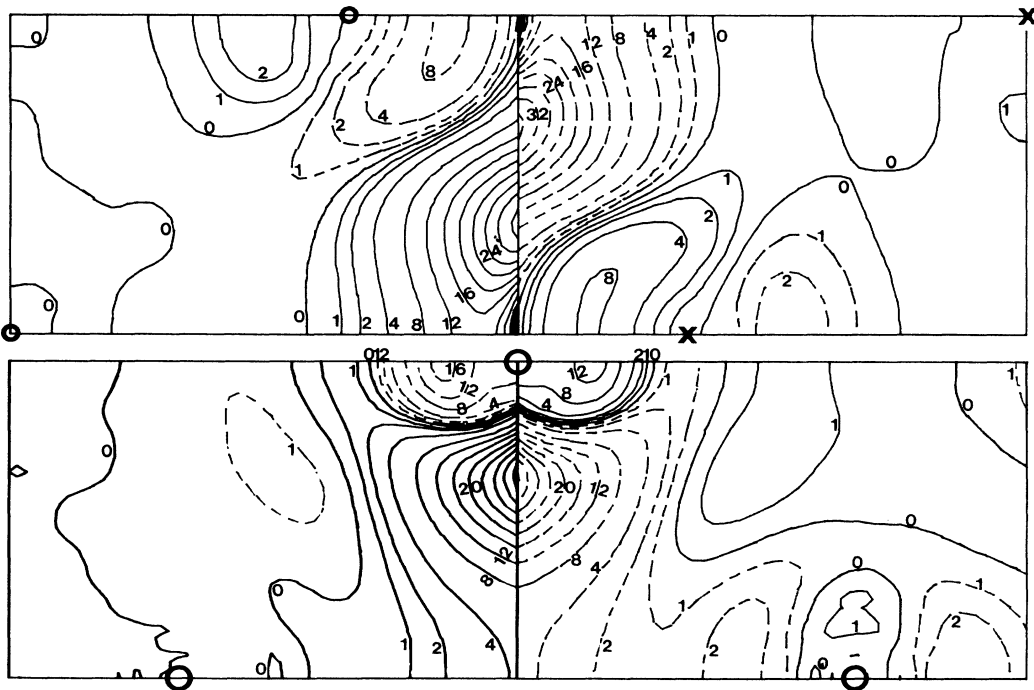


FIG. 1. Contours of constant $\Delta\rho = \rho_{\text{superlattice}} - \rho_{\text{constituent}}$ where $\rho_{\text{constituent}} = \rho_{\text{GaAs}}$ on one side of the midplane and ρ_{AlAs} on the other. The plots are in two (100) planes, one of which contain As atoms (large circles) and the other Ga atoms (small circles) and Al atoms (xs). Solid lines represent positive $\Delta\rho$ and dashed lines negative. The contours are 0, 1, 2, 4, 8, 12, 16, . . . in units of $2.5 \times 10^{-5} e^-/\text{bohr}^3$. There is reflection symmetry about the perimeters of the plots which cover a quarter of a unit cell (except that the edges of the As plane which have no atom on them have glide symmetry).

over the central layer of each three-layer side of the superlattice), but as we have seen, charge flows from AlAs to GaAs. The corresponding figure of Van de Walle and Martin¹⁵ used the p pseudopotential. They obtained $\Delta\bar{V}=0.032$ eV, but still in the wrong direction. Perhaps if an average over s and p pseudopotentials were used, a $\Delta\bar{V}$ of the correct sign would be obtained. The physical $\Delta\bar{V}$ should be small, however, because it is screened by the charge flow. Because of the deeper core potential of Ga, if an all-electron potential were used, a $\Delta\bar{V}$ of the correct sign to account for the charge flow would be obtained. But the valence electrons also have an extra node in the Ga core (relative to Al) so that it is not the all-electron $\Delta\bar{V}$, but rather some averaged pseudopotential $\Delta\bar{V}$ that controls the charge flow. In any event, by calculating the top of the valence band at Γ in bulk GaAs and AlAs (both with the superlattice lattice constant which is their average equilibrium lattice constant) relative to the \bar{V} s in these crystals and adding these to the corresponding \bar{V} s in Fig. 5 we obtain the valence-band offset $\Delta E_v=0.4456$ eV. The fully relativistic pseudopotential including a spin orbit was used to calculate the Γ_8 state at the top of the valence band without the

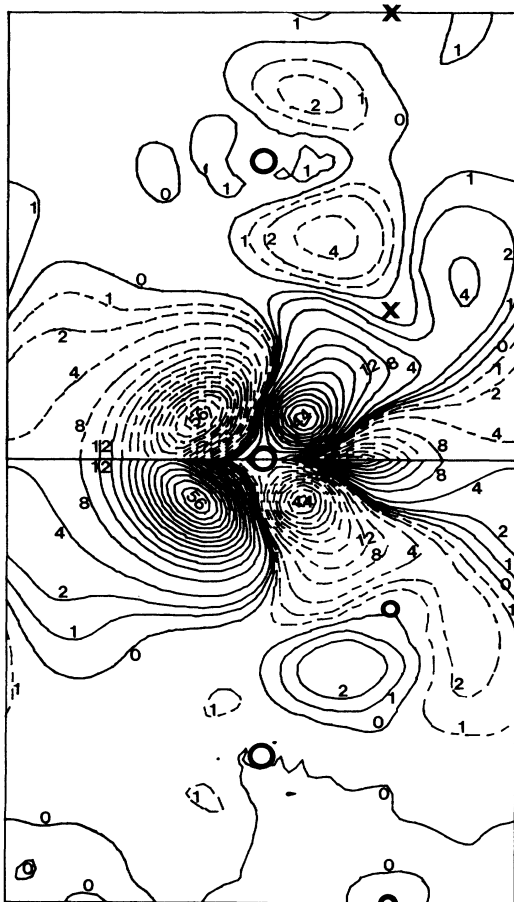


FIG. 2. Contours of constant $\Delta\rho$ in the (011) plane. There is reflection symmetry about the end planes (parallel to the mid-plane) of the plot which covers half a unit cell. Otherwise caption to Fig. 1 applies.

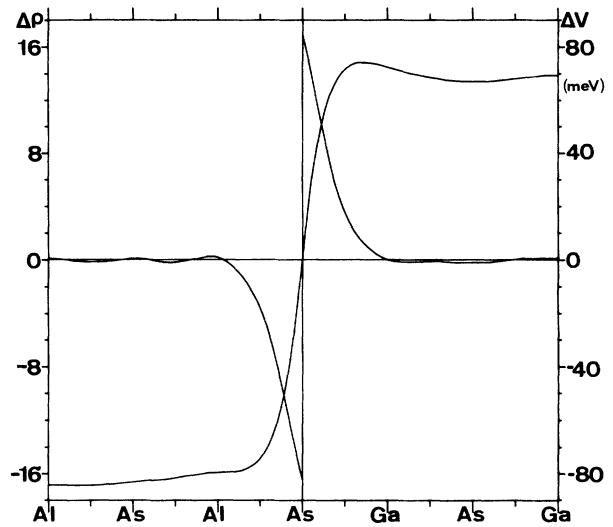


FIG. 3. Plot of the planar average $\Delta\rho$ in units of $2.5 \times 10^{-5} e^-/\text{bohr}^3$ and the double-layer potential ΔV it engenders in meV.

use of perturbation theory but using the self-consistent potential obtained with the scalar relativistic pseudopotential. This contributed 0.0146 eV to the ΔE_v quoted above, somewhat less than the 0.02 eV found in Ref. 15. We recalculated ΔE_v , replacing \bar{V} with \hat{V} where \hat{V} is the planar averaged local potential at the very center of each three-layer side of the superlattice. From the values of

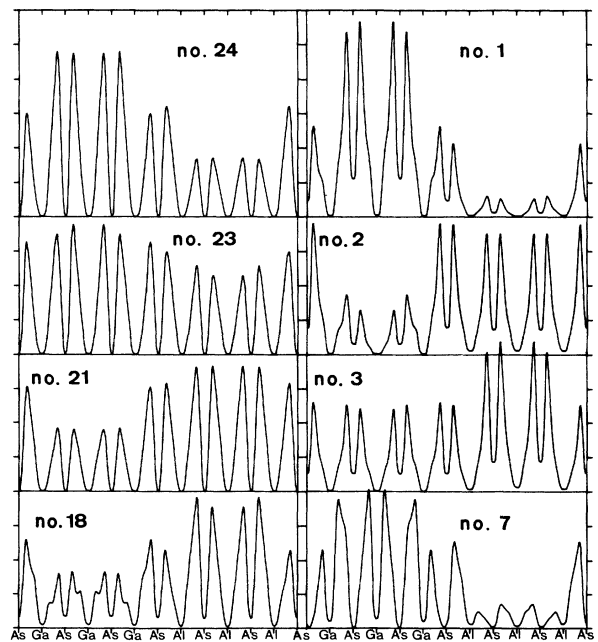


FIG. 4. Plots of $|\Psi_{\mathbf{k}}|^2$ averaged over the star of $\mathbf{k}=(2\pi/a)(\frac{1}{8}, \frac{1}{8}, \frac{1}{12})$ in arbitrary but identical units. The eight most localized (of the 24 valence states at \mathbf{k}) have been plotted along a zigzag path of atomic neighbor to atomic neighbor through the unit cell. The states are ordered from No. 1 at the bottom of the valence bands to No. 24 at the top.

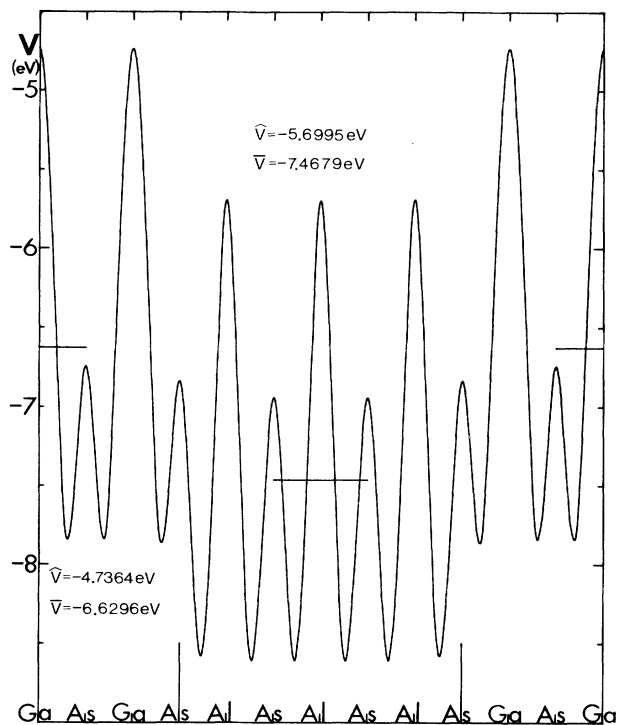


FIG. 5. Planar average of the local potential of the superlattice in eV. The horizontal lines represent \bar{V} , which is V averaged over the central cells. \hat{V} is V at the central Al and Ga planes.

\bar{V} and \hat{V} shown in Fig. 5 one can see that $\Delta\hat{V}$ differs from $\Delta\bar{V}$ by 0.2148 eV but its use results in $\Delta E_v = 0.4465$ eV. This 0.9-meV discrepancy is a consequence of using only three layers in the superlattice. Thus for all practical purposes the calculation is converged in cell thickness as well as \mathbf{k} -space sampling and almost converged in basis-set size. We previously estimated this error to be less than 8.5 meV.

After the pseudopotential used in Fig. 5 has been defined, there still remains an arbitrary zero of Coulomb potential so that, although $\Delta\bar{V}$ and $\Delta\hat{V}$ are meaningful, the \bar{V} and \hat{V} themselves are not. In an ideal world one could define a zero of Coulomb potential such that when the \bar{V} or \hat{V} of the bulk crystals were calculated, the correct $\Delta\bar{V}$ or $\Delta\hat{V}$ would be obtained without performing the superlattice calculation. Thus the band offset would simply be the difference in the Γ_8 levels of the two constituents. We have tried several ways to define the Coulomb zero of potential without success and it is our opinion that no such definition exists which will be successful for all superlattices. We can, however, define a zero of Coulomb potential which leads to a precise definition of the interfacial double layer, or dipole,²⁴ and when that dipole correction is added yields the exact valence-band offset. There does not appear to be any way to obtain the dipole correction without a superlattice calculation, so nothing is gained computationally. However, we have changed the question from one which has no answer, "What should we line up in the two constituents to obtain the correct band offset?" to one which has a precise, if not predictable

answer, "What is the potential across the interfacial double layer?"

Construct the (001) planar average of the pseudocharge density plus valence charge point ions of bulk GaAs. This $\rho(z)$ then consists of positive δ functions of alternating strengths 5 and 3 embedded in a compensating negative background. Now form a slab by slicing this planar averaged crystal through two As planes so that the two surface planes contain δ functions of strengths $\frac{5}{2}$. This electrically neutral slab has no dipole because the central Ga plane is a reflection plane. The potential at either surface is zero since it requires no work to bring an electron in from infinity to the surface. Then form AlAs slabs in an identical manner and construct the planar averaged zeroth-order superlattice by stacking alternate AlAs and GaAs slabs. The potential of a pair of these slabs is shown in Fig. 6. The potential is zero by construction at the As planes, has cusps at the planes because of their δ -function nature, and is positive everywhere because an electron upon entering the slab encounters forces to oppose its motion, both from the positive surface δ function behind it and the negative charge in front of it. The long horizontal lines in the figure represent \bar{V}_{Coul} , the average Coulomb potential on either side of the interface. The shorter horizontal lines represent the energy of the top of the valence bands in the bulk crystals when the arbitrary constant in the Coulomb potential is fixed to be consistent with this picture, i.e., when the planar average of the bulk Coulomb potential is set equal to zero on As planes. If our zeroth-order superlattice were exact, we could then obtain ΔE_v from calculations involving the bulk constitu-

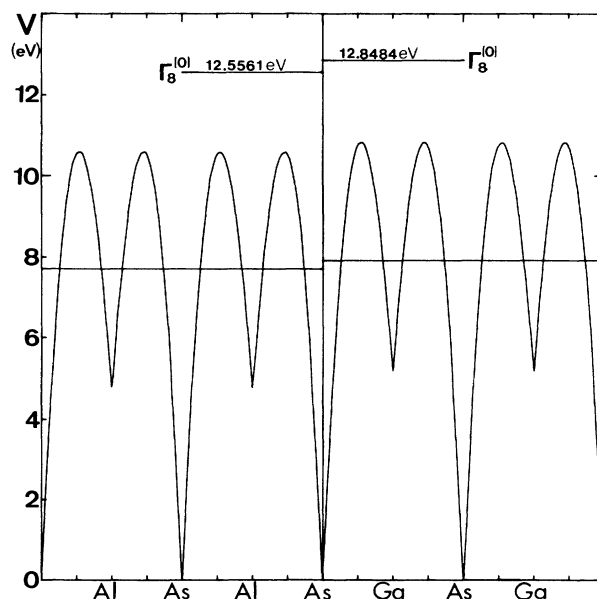


FIG. 6. Planar average of Coulomb potential arising from point ions and bulk pseudocharge densities of GaAs and AlAs as described in the text (in eV). The long horizontal lines represent the average of these potentials (7.7119 eV for AlAs and 7.9139 eV for GaAs). The shorter lines represent the tops of the valence bands when the zero of Coulomb potential is chosen according to this prescription.

ent crystals only. But our zeroth-order superlattice has a discontinuous charge density at the interface so charge must flow if for no other reason than to become continuous. Note that charge flow is just the planar average of the difference between the calculated superlattice charge density and that of its constituents which we have already plotted in Fig. 3 along with ΔV , the double-layer potential it engenders. Taking Δ_{dipole} to be the difference between ΔV at the center of the GaAs and AlAs layers, i.e., at the edges of Fig. 3, we have²⁵

$$\begin{aligned}\Delta E_v &= \Gamma_8(\text{GaAs}) - \Gamma_8(\text{AlAs}) \\ &= \Gamma_8^{(0)}(\text{GaAs}) - \Gamma_8^{(0)}(\text{AlAs}) + \Delta_{\text{dipole}} \\ &= 12.8484 - 12.5661 + 0.1538 = 0.4461 \text{ eV} .\end{aligned}$$

Although the exact determination of Δ_{dipole} requires a superlattice calculation, the charge discontinuity of $0.834 \times 10^{-3} e^-/\text{bohr}^3$ at the central plane of Fig. 3 is a bulk constituent difference. It might be possible to obtain a crude estimate of Δ_{dipole} from this discontinuity or from a knowledge of the electronegativities of the constituent atoms.

Since for a (001) strain the position of the atomic planes is determined from bulk elastic constants, the model is directly applicable to lattice-mismatched superlattices. Note, however, that it cannot be applied to a superlattice like $(\text{InAs})_n(\text{GaSb})_m$ (001) whose constituents have no common ion.²⁶ The model can be applied to (110) superlattices with or without a common ion. Because every (110) plane of ions in the bulk crystal contains both anions and cations, the slabs must be cut at the midplane point. Stacking slabs which have been cut between rather than through ion planes to form the superlattice will result in different charge discontinuity and a different Δ_{dipole} . It seems highly unlikely to us that

there can exist a single relationship between Δ_{dipole} and the zeroth-order charge discontinuity which is valid for both (001) and (110) superlattices.

In conclusion, we have performed what we believe to be the most accurate calculation yet of the valence-band offset in GaAs-AlAs(001) and obtained 0.446 eV, which is in excellent agreement with the most recent experimental results. We showed how this could be obtained from bulk constituent Γ_8 eigenvalues plus a precisely defined interfacial double-layer potential difference. We have also made an extremely accurate and, as far as we know, the only calculation of the formation enthalpy of $(\text{GaAs})_3(\text{AlAs})_3$. Of the three major sources of error in the calculation we estimate the Gaussian basis set to cause an error of less than +1.2 meV (three times the calculated discrepancy between the Gaussian basis and fully converged mixed-basis-set results for the monolayer superlattice), the random point sampling in real space to cause ± 0.5 meV and the finite k -space sample to cause ± 0.1 meV. The calculated 1.2-meV formation enthalpy per unit cell corresponds to 0.6 meV per interface compared with 7.45 meV per interface for the monolayer superlattice. This difference we attributed to Coulomb repulsion between interfaces and this implies that the completely isolated interface might actually have a negative formation enthalpy. This result we believe is important since earlier works^{14,27} involving monolayer superlattices gave at least the strong implication that the isolated interface had a small but definitely positive formation enthalpy and hence is only metastable.

ACKNOWLEDGMENTS

This work was supported by the Robert A. Welch Foundation (Houston, TX) and the National Science Foundation under Grant No. DMR-84-12408.

¹R. Dingle, W. Wiegmann, and C. H. Henry, *Phys. Rev. Lett.* **33**, 827 (1974).

²H. Kroemer, in *Proceedings of the NATO Advanced Study Institute on Molecular Beam Epitaxy and Heterostructures, Erice, Sicily, 1983*, edited by L. L. Chang and K. Ploog (Martinus Nijhoff, The Netherlands, 1985).

³R. S. Bauer and G. Margaritondo, *Physics Today* **40**, 27 (1987).

⁴W. I. Wang and F. Stern, *J. Vac. Sci. Technol. B* **3**, 1280 (1985).

⁵J. Menendez, A. Pinczuk, D. J. Werder, A. C. Gossard, and J. H. English, *Phys. Rev. B* **33**, 8863 (1986).

⁶D. Arnold, A. Ketterson, T. Henderson, J. Klem, and H. Morokoc, *J. Appl. Phys.* **57**, 2880 (1985).

⁷J. L. Shay, S. Wagner, and J. C. Phillips, *Appl. Phys. Lett.* **28**, 31 (1976).

⁸W. R. Frensley and H. Kroemer, *J. Vac. Sci. Technol.* **13**, 810 (1976).

⁹W. A. Harrison, *Electronic Structure and Properties of Solids* (Freeman, San Francisco, 1980), p. 253.

¹⁰C. G. Van de Walle and R. M. Martin, *J. Vac. Sci. Technol. B* **4**, 1055 (1986).

¹¹R. Latter, *Phys. Rev.* **99**, 510 (1955).

¹²J. Tersoff, *Phys. Rev. B* **30**, 4874 (1984); *Surf. Sci.* **168**, 275 (1986).

¹³M. Jaros, K. B. Wong, and M. A. Gell, *Phys. Rev. B* **31**, 1205 (1985).

¹⁴D. M. Bylander and L. Kleinman, *Phys. Rev. B* **34**, 5280 (1986).

¹⁵C. G. Van de Walle and R. M. Martin, in *Computer-Based Microscopic Description of the Structure and Properties of Materials* (Materials Research Society, Pittsburgh, 1986), Vol. 63.

¹⁶W. E. Pickett, S. G. Louie, and M. L. Cohen, *Phys. Rev. B* **17**, 815 (1978).

¹⁷Note that type-III crystal harmonics listed in Table II of Ref. 14 occur on cations (except for those on central planes) as well as on anions in three-layer superlattices.

¹⁸The twelve- k -point sample of the superlattice BZ is identical to the usual ten-point sample of the fcc BZ as discussed in Ref. 14.

¹⁹A positive value of the formation enthalpy means the superlattice is unstable with respect to phase separation.

²⁰The large discrepancy with experiment in the cohesive energy

is a consequence of the large difference in atomic and crystal local-density-approximation errors. These LDA errors are completely negligible when crystal energies are compared with crystal energies in either the valence-band-offset or formation-enthalpy calculations. Because the LDA yields extremely poor semiconductor energy gaps, a direct calculation of conduction-band offsets would be hopeless.

²¹Y. T. Shen, D. M. Bylander, and L. Kleinman, *Phys. Rev. B* **36**, 3465 (1987).

²²This is half of the energy per unit cell since each cell contains two interfaces, one in the center and one-half on each end.

²³L. Kleinman and D. M. Bylander, *Phys. Rev. Lett.* **48**, 1425 (1982).

²⁴The terms surface dipole and interfacial dipole as used in the literature are, more often than not, meaningless. These dipoles are due to the rearrangement of charge, but, unless the original charge distribution from which the charge was rearranged is explicitly defined, the dipole itself is undefined.

²⁵The attentive reader will note that this result lies between the results obtained previously using $\Delta\bar{V}$ and $\Delta\hat{V}$ and may think it should agree with $\Delta\hat{V}$ since Δ_{dipole} and $\Delta\hat{V}$ both represent central plane differences whereas $\Delta\bar{V}$ is a central cell difference.

However, V contains exchange as well as Coulomb contributions so all that can be expected is that the agreement between all three results gets better as the superlattice gets thicker.

²⁶The slabs must be cut from the bulk crystal at planes which lie between ion planes in this case. Because the slabs have no reflection plane, there is no unique way to do this. There are two kinds of interfaces (Sb-In and As-Ga) which individually cannot be expected to be electrically neutral so that there will be long-range electric fields in the superlattice. One can avoid this difficulty by having an extra plane of anions in one slab and an extra plane of cations in the other, for example $(\text{In}_{n+1}\text{As}_n)(\text{Ga}_m\text{Sb}_{m+1})$. Then there is only one kind of interface, the slabs cut from the bulk crystal have reflection symmetry, and they can be made electrically neutral by cutting the bulk crystals at the appropriate place between anion and cation planes. This cut of the bulk crystals then results in a spacing between the In and Sb planes on either side of the interface which should be close to, but not exactly equal to, the actual spacing.

²⁷D. M. Wood, S.-H. Wei, and A. Zunger, *Phys. Rev. Lett.* **58**, 1123 (1987).